Journal of Engineering Sciences, Assiut University, Vol.35, No.2 pp.421-442, March 2007

CALIBRATING THE NONLINEAR ELASTIC AND VISCOELASTIC TISSUE PROPERTIES OF LEFT VENTRICULAR MUSCLE FROM GUINEA PIG HEART

M. A. Hassan

Mechanical Engineering Department, Faculty of Engineering, Assiut University, Assiut,71516 El_khozami@roketmail.com

(Received 22 November 2006 Accepted 27 January 2007)

Mechanical behavior of the heart muscle tissues is the central problem in finite element simulation of the heart mechanics. Nonlinear elastic and Viscoelastic behaviors and their constitutive relations are determined from experimental data in order to characterize the passive response of the left ventricular myocytes (muscle cells) taken from guinea pig heart. Uniaxial tension test was made to determine the constants of the nonlinear elastic model (hypoelastic) in which Eulerian or exponential stress-strain relationship was assumed to describe the passive response of the heart material. Nonlinear elastic behavior was also described by hyperelastic strain energy functions such as Ogden models and Mooney–Rivlin models and the corresponding energy functions coefficients were determined. Stress relaxation test was conducted to assess relaxation behavior as well as viscosity of the tissues. Viscohyperelastic behavior was constructed by a multiplicative decomposition of a standard Mooney-Rivlin or Ogden strain energy function, W *, for instantaneous deformation and a relaxation function,* $R(t)$*, in a Prony series form. Nonlinear least square fitting and constrained optimization was conducted under MATLAB and MARC in order to obtain the material constants. From the physics of heart motion we found that hypoelastic or hyperelastic behaviors could be safely used for heart mechanics simulation, because the characteristic relaxation time is very large compared with the actual time of heart beating cycle. To get more precise mechanical properties, needed for very accurate bio-simulation and development of new material for artificial heart, an optimization algorithm was proposed to correct and estimate material parameters from clinical intact heart measurements.*

KEYWORDS: *heart muscle, hypoelastic, hyperelastic, strain energy functions, viscohyperelastic*

1. INTRODUCTION

Finite element analysis is a powerful tool to construct a virtually living beating heart and studying heart mechanics [1]. For instance, from the FE-analysis we

can obtain huge data about cardiac motion, especially stress and strain of the heart that are two of the most important determinants of many cardiac physiological and pathophysiological functions. These functions include: the pumping performance of the ventricles; the oxygen demand of the myocardium; the distribution of coronary blood flow; the vulnerability of the regions to ischemia and infarction diseases; and the risk of arrhythmia [2].

There are four fundamental requirements or steps to derive and formulate the equation of motion of the heart. These are (1) kinematics relations, (2) stress equilibrium equations, (3) constitutive relations and (4) boundary conditions [3]. Constitutive relations or the experimental relationship between stress and strain is the central prerequisite demand in modeling heart mechanics using FE-method.

Biological tissues exhibit time dependence when subjected to relaxation test and hysteresis when subjected to cyclic loading. Previous studies have long controversy focused on which of the hypoelastic, hyperelastic, or viscoelastic are the dominant mechanical behaviors of the heart muscle, and which constitutive relation should be confidently used in heart FE-simulation. Strain energy functions like Mooney-Revilin and Ogden models are used for hyperelasticity [4, 5] while viscoelastic strain energy functions are used for viscoelasticity [6]. Nonlinear elastic (reversible) model in which Eulerian or exponential stress-strain relationship was assumed to describe the passive response of the tissue's material by nonlinear elastic relations known as hypoelastic behavior [7, 8].

There are several experimental techniques to assess the mechanical behaviors of the biological materials in vitro. Among these are indentation probes [9-11], tension [12] and compression [13] testers and rotary or cyclic shear tests [14]. Ultrasound electrograph [15] and magnetic resonance electrograph [16] become available techniques for in vivo tests, but in many cases the data obtained are not easily comparable. That is either because the tissue sample sizes employed or testing domain (strain and frequency range) are not comparable, or merely because of few tests conducted on the same tissues. In particular, magnetic resonance imaging MRI and tagging methods provide mostly global information about material properties and deformation of the heart.

In this paper, the author developed a very precise uniaxial and relaxation tests to determine the nonlinear elastic and viscous behaviors of the Guinea pig left ventricle myocardium (heart muscle). Nonlinear curve fitting and optimization using MATLAB tool box and MARC were conducted to determine model's constants that characterize the nonlinear elastic and viscous behavior of the heart tissues. The generalized strain energy function versus time data being used for large strain viscoelasticty was generated by using our experimental data; and our data mixed with equi-biaxial tension and volumetric compression (existing in [2], [3]) to determine constants of the myocardium

free energy function. However, stress relaxation tests at multiple levels of strains were conducted to generate the relaxation function. The results are discussed from, the mechanical, biomechnical and physiological point of views.

2. APPARATUS

The experimental apparatus was built on an optical microscope provided with Charge-Coupled Device (CCD) video camera as shown schematically in Fig.1. Myocardium (heart muscle) sample length in relaxed state was put on the sample holder and its initial length was measured from the picture appearing on the scaled monitor. The sample was attached at one end to a hook from a micrometer of the extensometer for controlling sample length and extension, and at the other end to a hook from a semiconductor strain gage sensor (F.S.) (Akers AE801; AME) for force measurement. The analogue force and displacement signals were amplified and recorded by the thermal array recorder before they were converted to digital signal, through a data acquisition system, and stored on a P.C. To minimize movement on the hook during extension, muscle sample was nodded by 000 nylon thread at the two ends. The sample measured length is the distance between the two nodes appeared on the scaled monitor. The electronic stimulator and digital oscilloscope are needed to provide the physiological, biophysical and electrical conditions similar to those of the intact heart. Figure 2 shows a photograph of the sample, sample holder, extensometer, and force sensor (F.S.).

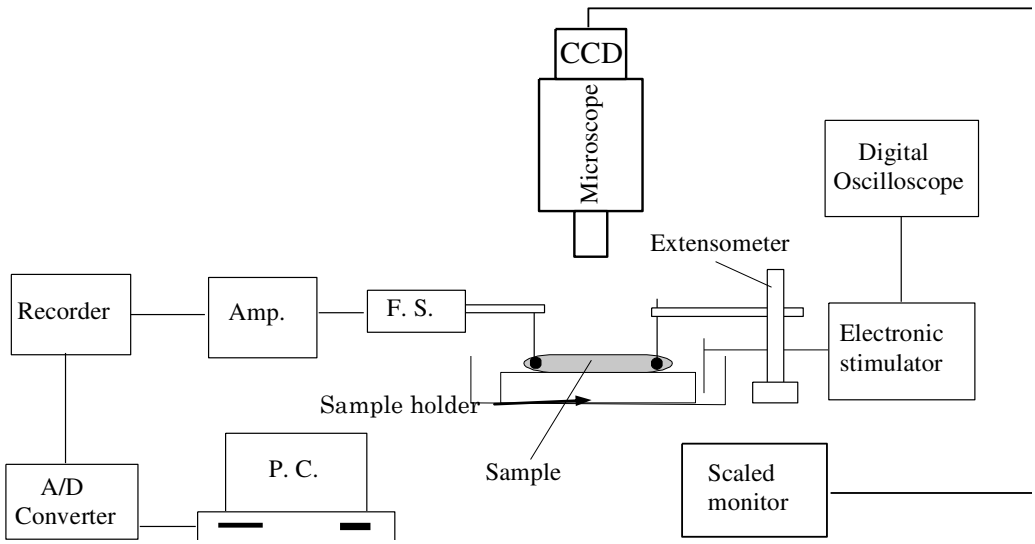

Fig.1 Schematic diagram of the experimental apparatus for uniaxial tension test

3. EXPERIMENTAL DETAILS

Guinea pigs (2kg) were anesthetized with an intravenous injection of sodium pentobarbital, incubated and ventilated. The pericardium opened, the ascending aorta cross-clamped, and the heart arrested with 50-150 ml intracardiac injection of an oxygenated low-sodium high potassium solution. The heart was removed and placed in a beaker containing this solution. The right ventricular free wall and intraventricular septum were excised with scissors, and left ventricular free wall was isolated. A trabicula papillary muscle was taken out to make samples of measured length 8 mm and cross sectional area 4 mm^2. During testing, the initial tension was set to zero, and strain was increased gradually till 50% tensile strain. This protocol was repeated five times for each sample and then followed by a relaxation test. Relaxation tests were made under10%, 20%, 30%, 35%, 40%, 45% and 50% constant strains. Although 12 specimens were tested, we reported only seven samples in which the sample size and fiber orientation was nearly the same on each test. All samples were tested at room temperature.

4. MATERIAL MODELS OF THE HEART TISSUES

4.1 HYPOELATICITY APPROACH

Used to model heart tissues as a nonlinear solid considering that the elastic modulus is dependent only on strain i.e. the elastic tangent modulus is linear in relation with stress. One way to describe this material behavior is the exponential model given by the empirical Eq. (1-a) where k and k_s are material constants determined from experiment.

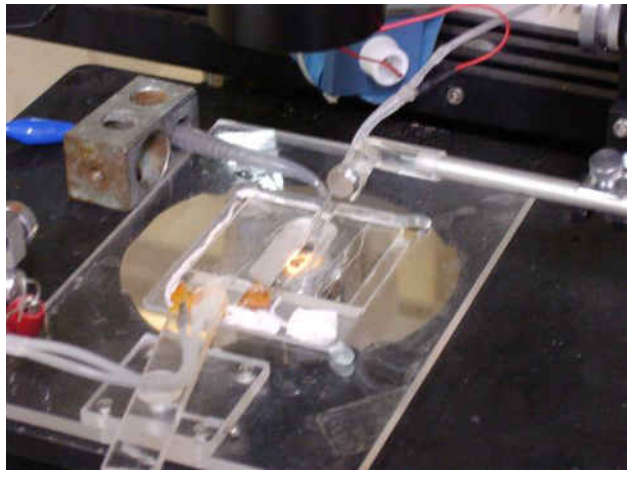

Fig. 2 Photograph of the setup for uniaxial tension test

$$\sigma = \frac{\mathrm{K_S}}{K}(\mathrm{e}^{\mathrm{k}\varepsilon} - 1) \tag{1-a}$$

$$E_t = k\sigma + k_s \tag{1-b}$$

4.2 HYPERELASTICITY APPROACH

For materials like rubbers and biological tissues are described by strain energy functions in order to guarantee that the rigid body motions play no role in the constitutive law. Mathematically, this is achieved by postulating the existence of a strain energy density function, W, to be a scalar potential that depends on the component of the right Cauchy-Green deformation tensor or Green's strain tensor. Components of the second Piola-Kirchhoff stress tensor are given by the derivatives of W with respect to the components of the Green's strain tensor. For isotropic hyperelastic material, the strain energy is constant for all orientations of the coordinate axes. Thus the strain energy is an invariant of Green' strain tensor, E, and can be expressed as a function of the three principal invariants of E as shown in Eq. (2) which is known as Mooney-Rivilin model.

$$W(E_{ij}) = W(I_1, I_2, I_3) = C_1(I_1 - 3) + C_2(I_2 - 3) + C_3(\frac{1}{I_3^2} - 1) + C_4(I_3 - 1)^2 \tag{2}$$

The constants C_3 and C_4 are related to C_1 and C_2 as;

$C_3 = \frac{1}{2}C_1 + C_2, C_4 = \frac{C_1(5v-2) + C_2(11v-5)}{2(1-2v)}$ where the Poisson's ratio $v = 0.49$.

The strain invariants I_1, I_2 and I_3 in terms of the principal stretch ratios, λ_1, λ_2 and λ_3 are defined as:

$$\begin{aligned} I_1 &= \lambda_1^2 + \lambda_2^2 + \lambda_3^2 \\ I_2 &= \lambda_1^2\lambda_2^2 + \lambda_2^2\lambda_3^2 + \lambda_3^2\lambda_1^2 \\ I_3 &= \lambda_1^2\lambda_2^2\lambda_3^2 \end{aligned} \tag{3}$$

In Eq. (2), C_1 and C_2 are material constants which must be determined experimentally. For complete incompressibility of the material, $I_3 = 1$. However, Spencer [17] noted that it is not sufficient to set $I_3 = 1$ in Eq. (2) since certain derivatives of W, tend to infinity in the limiting case of incompressibility. This problem is overcome by introducing the arbitrary constants C_3 and C_4. Also, in Eq. (2) it can be noted that the use of $(I_1 - 3)$ and $(I_2 - 3)$ ensures that the strain energy is zero when the strains are zeros. This can be easily explained, because for zero strains the principal stretch ratios $\lambda_1 = \lambda_2 = \lambda_3 = 1$ in which case Eq. (3) reduces to $I_1 = I_2 = 3$ and $I_3 = 1$.

4.3 VISCOHYPERELASTICITY APPROACH

For large strain viscoleastic material the strain energy function becomes

$$\psi\left(E_{ij},Q_{ij}^{n}\right)=\psi\left(I_1,I_2,I_3,Q_{ij}^{n}\right)=W\left(E_{ij}\right)-\sum_{n=1}^{N}Q_{ij}^{n}E_{ij}+\sum_{n=1}^{N}W_1^{n}\left(Q_{ij}^{n}\right) \tag{4}$$

where E_{ij} are the components of the Green's strain tensor, Q_{ij} internal variables and W the elastic strain energy density for instantaneous deformations. The components of the second Piola-Kirchhoff stress are given as

$$S_{ij}=\frac{\partial\psi}{\partial E_{ij}}=\frac{\partial W}{\partial E_{ij}}-\sum_{n=1}^{N}Q_{ij}^{n} \tag{5}$$

Equation (4) can also be written in terms of the long term moduli resulting in a different set of internal variables T_{ij}^{n} as shown in Eq. (6).

$$\psi\left(E_{ij},T_{ij}^{n}\right)=\psi^{\infty}\left(E_{ij}\right)+\sum_{n=1}^{N}T_{ij}^{n}E_{ij} \tag{6}$$

where ψ^{∞} is the elastic strain energy for long term deformations. Using this energy function definition, the stresses are obtained from Eq. (7) as;

$$S_{ij}=\frac{\partial\psi}{\partial E_{ij}}=\frac{\partial\psi^{\infty}}{\partial E_{ij}}+\sum_{n=1}^{N}T_{ij}^{n} \tag{7}$$

The viscoelastic energy function, Eq. (6) can also be expressed as Prony series expansion with similar form of each term as;

$$\psi=\psi^{\infty}+\sum_{n=1}^{N}\delta^{n}W\exp\left(-t/\lambda^{n}\right) \tag{8}$$

Where δ^{n} time dependent scalar multipliers and λ^{n} associated relaxation times. At time zero (or for time process: $t<\lambda^{n}$), the elastic energy of Eq. (8) reduces to:

$$\psi(0)=W=\psi^{\infty}+\sum_{n=1}^{N}\delta^{n}W \qquad \text{Or} \quad \psi^{\infty}=\left[1-\sum_{n=1}^{N}\delta^{n}\right]W \tag{9}$$

Then the time dependent energy function is given by substitution of Eq. (9) into Eq. (8) as:

$$\psi(t) = W\left[1 - \sum_{n=1}^{N} \delta^n \left(1 - \exp\left(-t/\lambda^n\right)\right)\right] \tag{10}$$

If we restrict ourselves for the simplicity of the discussion to the case N=2 we have: $\psi^{\infty} = \left[1 - \delta^1 - \delta^2\right]W$

$$\psi(t) = W\left[1 - \delta^1\left(1 - \exp\left(-t/\lambda^1\right)\right) - \delta^2\left(1 - \exp\left(-t/\lambda^2\right)\right)\right] \tag{11}$$

The energy function, $\psi(t)$ versus time data being used for viscohyperelasticity can be generated by fitting the experimental data provided by the following two tests: (i) Standard quasi-static tests (tensile, equi-biaxial tension and volumetric compreesion) to determine the material constants (i.e. C_1 , C_2 , C_3 and C_4 in Eq. (2) of the free energy function W, (ii) Standard relaxation tests to obtain scalar multipliers, δ^1, δ^2 and relaxation time constants, λ^1, λ^2.

5. HEART MECHANICAL CYCLE

The blood pressure versus blood volume in the left ventricle cavity in the heart cycle is shown schematically in Fig. 3. The diagram has many advantages, but in FE-simulation the four phases of the cardiac pressure cycle become very useful if they are illustrated as a function of time as shown schematically in Fig. 4. In these two figures the mitral valve closes at A and the left ventricle undergoes isovolumic contraction; muscle generate rapid contractile force while blood volume is constant therefore blood pressure is rapidly rising until B. when the left ventricular pressure exceeds the aortic pressure and the aortic valve opens, blood is ejected to the aorta and left ventricle volume begins to decrease. The aortic valve closes at the end of systole C because the muscle starts to relax and intraventricular pressure falls below the aortic pressure. The left ventricular muscles then undergo isovolumic relaxation from C to D. The mitral valve reopens at D when the pressure of left ventricular is lower than that of left atrium. Blood pressure in right ventricle changes in a similar manner over the heart contraction cycle, but its magnitude is about three times smaller than that of the left ventricle [19]. The total time of this cycle is 800 ms and that is why the heart beats is 75 /min. The work done by the left ventricle in one cycle is the area enclosed in the loop ABCD.

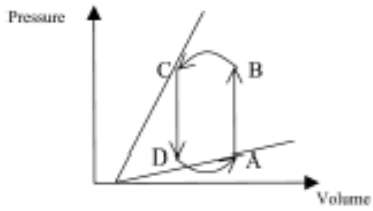

Fig. 3 Schematic ventricular pressure-volume loop

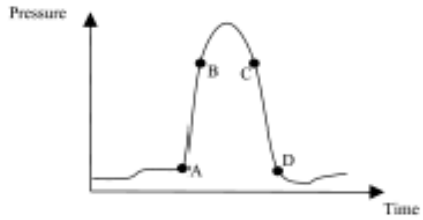

Fig. 4 Ventricular pressure changes over time

6. RESULTS AND DISCUSSION

6.1 HYPOELASTIC MATERIAL CONSTANTS (KS AND K)

Figure 5, shows the true stress versus true strain obtained from uniaxial test for seven samples taken from left ventricle guinea pig heart. The experimental data are fitted to the hypoelastic model using Eq. (1) and the corresponding material constants K_s and K are obtained and listed in Table 1. The heart tissues show a very steep rise in stress as the strain is approaching the limiting strain for elastic response (normally it is taken 60% strain). Equation (1-a) is very useful in hypoelasticity because polynomial functions are not appropriate as they do not model this singular behavior. Figure 6 shows the engineering stress versus stretching ratio, λ, for the same seven samples. To prevent irreversible damage (plastic strain), the samples were not stretched beyond stretch ratio $\lambda = 1.72$ (0.54 strain). To implement these results in finite element code, we need only to update elasticity matrix (matrix relating stress with strain). Since the components of the elasticity matrix are functions of Poission ratio and elastic modulus, therefore the tangent modulus, E_t, at the end of each strain increment must be updated using Eq. (1-b). This technique was implemented in the author FE C-code as well as in Marc and the simulation results have been published in [2004]

6.2 RELAXATION TIME CONSTANT (τ_R)

Figure 7 shows the experimental stress relaxation versus time at different strain levels ranging from 0.1 to 0.5 for seven samples during 90 seconds testing time. Based on Maxwell element model, the stress at any time, t required to maintain the strain constant is given by $\sigma = \sigma_o \, e^{-t/\tau_R}$ which was used for curve fitting. The experimental data were fitted to the previous equation to determine the relaxation time τ_R which is equal to μ/G, where μ is the viscosity

coefficient and G is the elastic shear modulus. Tables 2,3 and 4 list the values of μ, G and τ_R for the all data (from 0-90s), long term data (from 7-90s) and short term data (0-7s), respectively. For short term data, the obtained relaxation time $(\tau_{Rave} = 666.2521s)$ is very large compared with the heart cycle time (800ms) which means that the heart muscle contracts very fast before any significant relaxation takes place. Therefore stress relaxation in heart muscle is very small and could be ignored confidently in simulation of the heart mechanics. For the long term data (from 7- 90s) the seven samples demonstrate non-significant decrease in stress versus time and a significant decrease in the rate of stress relaxation with increasing strain were observed. The average relation time for long term data was 56.2774s while it was 445.2925s for all data fitting. In the short term data region, the samples show slightly increase in the stress relaxation rate with increasing strain level. The average value of the muscle viscosity 17 s.N/mm^2 indicates a small damping ratio and the muscle tends to behave like solid rubber material.

Table 1 Summery of K_s and K values, Eq.(1)

Test No.	*K_s – Value mN/mm2*	*K – Value (constant)*
1	6.8953	2.6145
2	6.6760	1.7961
3	9.3707	9.4015
4	9.3832	10.0050
5	9.2901	7.3226
6	10.7959	19.4881
7	*10.8280*	*24.5970*

6.3 HYPERELASTIC MODELS (ENERGY FUNCTIONS)

6.3.1 FIRST ORDER MOONEY-RIVLIN ENERGY FUNCTION

Since the constants C_3 and C_4 in Eq. (2) are dependent it can be easily determined if we know the constants C_1 and C_2. Because, heart tissues are nearly incompressible, the principal stretches in uniaxial test are then given by $\lambda_1 = \lambda_t$, $\lambda_2 = \lambda_3 = \frac{1}{\sqrt{\lambda_t}}$ and the logarithmic stress in axial direction is given

by $\sigma_1 = \sigma_t = \lambda_1 \dfrac{\partial W}{\partial \lambda_1} = 2C_1\left(\lambda_t^2 - 1\right) + 4C_2\left(\lambda_t - 1\right);$ (11)

and the corresponding engineering stress is given by

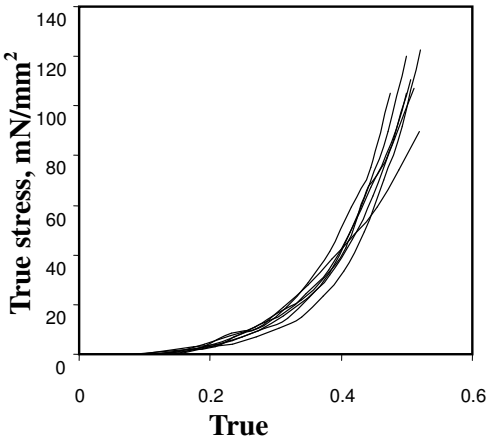

Fig. 5 Experimental true stress versus true strain

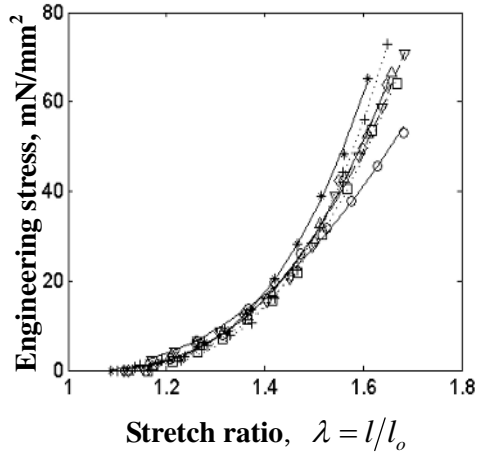

Fig. 6 Experimental Engineering stress versus stretching

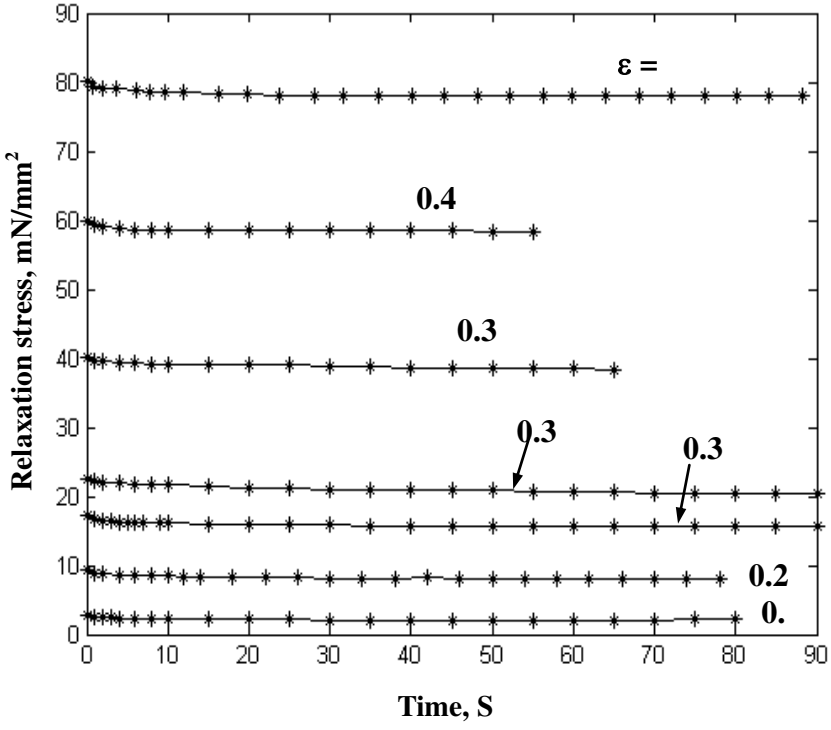

Fig. 7 Results of the relaxation test under various strain levels

Table 2 Viscosity and relaxation time for all data fitting (0-90s)

Sample No.	Elastic modulus E (N/mm2)	Viscosity (N/mm2.S)	Shear modulus G (N/mm2)	Relaxation time, τ_R(s)
1	0.1700	22.8159	0.0570	400.2789
2	0.1080	16.4096	0.0362	453.3038
3	0.0913	16.5826	0.0306	541.9150
4	0.1585	16.6015	0.0532	312.0582
5	0.1577	16.2005	0.0529	306.2476
6	0.0743	16.1494	0.0249	648.5702
7	0.1049	16.0538	0.0352	456.0738

Table 3 Viscosity and relaxation time for long –term data fitting (7-90s)

Sample No.	Elastic modulus E (N/mm2)	Viscosity (N/mm2.S)	Shear modulus G (N/mm2)	Relaxation time, τ_R(s)
1	2.0492	28.3322	0.6876	41.2044
2	1.6392	26.5065	0.5501	48.1848
3	3.7575	56.1087	1.2609	44.4989
4	1.8991	36.4060	0.6373	57.1253
5	2.0665	42.5920	0.6935	61.4160
6	0.7304	15.7698	0.2451	64.3402
7	0.5489	14.8534	0.1842	80.6373

$$S_1 = S_t = \frac{\sigma_1}{\lambda_t} = 2C_1\left(\lambda_t - 1\right) + 4C_2\left(1 - \frac{1}{\lambda_t}\right)$$

where, λ_t is the stretch ratio in uniaxial test.

We substitute the experimental values into Eq. (11) and solve by means of nonlinear least square method using Lvenberg-Marquradt nonlinear curve fitting algorithm under MTALB optimization tool box. The problem was solved

by means of Marc optimization toolbox in Mentat. The obtained results values are shown in Table 5. The constants often turned negative and therefore physically are not meaningful. This phenomenon is a numerical hardship i.e. negative constants are just values obtained from good fitting and not the fundamental material behavior. In another words, these numerical values are just constants of the energy function to be used in finite element simulations regardless of their negative singe.

Table 4 Viscosity and relaxation time for short-term data fitting (0-7s)

Sample No.	Elastic modulus E (N/mm2)	Viscosity (N/mm2.S)	Shear modulus G (N/mm2)	Relaxation time, τ_R (s)
1	0.1023	32.0208	0.0343	933.5510
2	0.0465	13.8432	0.0156	887.3846
3	0.0496	14.3671	0.0166	865.4879
4	0.1152	16.2898	0.0386	422.0155
5	0.1637	22.2671	0.0549	405.5938
6	0.0362	17.8446	0.0121	1474.7603
7	0.0842	15.2950	0.0283	540.4593

Table 5 Material constants obtained by tension tests with Mooney Model Eq. (11)

Sample	Material constants			
	C_1	C_2	C_3	C_4
1	45.5837	-49.9435	-2.1799	25.8675
2	47.3025	-50.7251	-1.7113	37.5834
3	38.588	-41.5288	-1.4704	29.2092
4	60.8695	-67.4353	-3.2829	27.2877
5	63.8834	-70.3662	-3.2414	32.6178
6	97.7597	-110.7	-6.4702	20.4716
7	80.444	-91.4945	-5.5252	12.9236

6.3.2 SECOND ORDER MOONEY –RIVLIN ENERGY FUNCTION

In order to obtain a good fitting with the experimental data, other Mooney-Rivlin model called the second order invariant energy function is used. In this model the energy function has four independent material constants as shown in equation

$$W = C_{10}(I_1 - 3) + C_{01}(I_2 - 3) + C_{11}(I_1 - 3)(I_2 - 3) + C_{20}(I_1 - 3)^2 \qquad (14)$$

The constants C_{10}, C_{01}, C_{11} and C_{20} for the seven samples are listed in Table 6.

Table 6 Material constants of the Mooney second order model, Eq.(14)

Sample	Material constants			
	C_{10}	C_{01}	C_{11}	C_{20}
1	901.73	-989.845	-1247.72	704.307
2	115.333	-118.983	-506.401	374.867
3	-35.7247	40.7749	-228.505	217.773
4	-92.0673	99.946	-34.3133	84.9795
5	-88.3484	95.4644	-0.711579	58.3431
6	-3.96832	2.86042	-57.8437	75.7684
7	136.724	-145.628	-438.653	318.694

6.3.3 SLIGHTLY COMPRESSIBLE ENERGY FUNCTION

In this model, the heart tissues are taken to be virtually incompressible and slightly compressible. Such energy function is given by the following formula called Ogden model.

$$W = \sum_{n=1}^{N} \frac{\mu_n}{\alpha_n}\left[J^{\frac{-\alpha_n}{3}}\left(\lambda_1^{\alpha_n} + \lambda_1^{\alpha_n} + \lambda_1^{\alpha_n}\right) - 3 \right] + 4.5K\left(J^{\frac{1}{3}} - 1 \right)^2 \qquad (15)$$

where, μ_n and α_n are material constants, K is the initial bulk modulus, and J is the volumetric ratio defined by $J = \lambda_1\lambda_2\lambda_2$ where λ_1, λ_2 and λ_3 are the

principal stretch ratios. The order of magnitude of the volumetric changes per unit volume should be 0.01[17]. Usually, the number of terms taken into account in the Ogden models is $N=2$ or $N=3$. Heart Material constants obtained from fitting experimental tension tests with Ogden Model (Eq. 15) are listed in Table.7.

The Ogden model is different from the Mooney-Rivlin model in several respects. The Mooney material model is defined with respect to the invariants of the right or left Cauchy-Green strain tensor and implicitly assumes that the material is incompressible. The Ogden formulation is defined with respect to the eigenvalues of the right or left Cauchy-Green strain, and the presence of the bulk modulus implies some compressibility. Using a two-term series ($N=2$) results are in identical behavior as the Mooney mode if: $\mu_1 = 2C_{10}$, $\alpha_1 = 2$, $\mu_2 = -2C_{01}$ and $\alpha_2 = -2$.

Table 7 Material constants of Eq.(15) obtained by experimental tension test.

Sample	Material constants		Exponents		Bulk modulus, K
	μ_1	μ_2	α_1	α_2	
1	0.165099	0.120588	6.07525	17.5329	7793.21
2	0.802652	0.168456	1.81091	17.2524	10899.5
3	9.0895e-6	0.122669	8.23129	18.7237	5742.07
4	0.155817	2.5933e-6	17.4716	1.93636	6805.97
5	3.1452e-6	0.184943	14.9739	17.0188	7868.91
6	0.430376	1.1435e-6	14.1682	11.3681	15244.2
7	1.1691e-7	0.195871	19.5630	16.5728	8115.31

6.4 PARAMETERS δ AND λ OF THE RELAXATION FUNCTION

In section (4.3), viscohyperelastic energy function is given by Eq. (10) or (11) which are based on a multiplicative decomposition of a standard Mooney-Rivilin or Ogden form strain energy function, W, for instantaneous deformation and a relaxation function $R(t)$, in a Prony series form Eq. (16).

$$R(t) = 1 - \sum_{n=1}^{N} \delta^n \left(1 - \exp\left(-t/\lambda^n\right)\right) \tag{16}$$

From equation (16) the relaxation function (for N=2) is stated as;

$$R(t) = \left[1 - \delta^1\left(1 - \exp\left(-t/\lambda^1\right)\right) - \delta^2\left(1 - \exp\left(-t/\lambda^2\right)\right)\right] \tag{16-a}$$

Fitting the relaxation experimental data with the relaxation function, $R(t)$, the four parameters λ^1, λ^2 □ δ^1 and δ^2 are obtained and listed in Table 8. According to experiments, the relaxation function $R(t)$ was assigned two relation terms; one (λ^1, δ^1) for fast relaxation and the other (λ^2, δ^2) for slow relaxation where λ^n is a nondimensional multiplier and δ^n is the associated time constant.

7. EFFECT OF AMOUNT OF INFORMATION ON THE CONSTANTS OF THE ENERGY FUNCTIONS

We conducted a series of fits for Mooney Rivlin model (Eq. (2)) that used progressively more information as the basis for the curve fitting. Mixed biaxial and volumetric compression data taken from literature [1,4] is used together with our uniaxial experimental data to assess the constants of Eq. (2). Table 9 summarizes the constants calculated in each case. The conclusion is that adding biaxial data to the uniaxial data had a strong influence on the quality of the fit and changed the constants greatly. However, adding further volumetric compression data has no effect on the calculated constants. Also we conducted a series of Ogden 2-term fits that used uniaxial data, uniaxial plus biaxial data, and uniaxial plus biaxial plus volumetric compression data as the basis for the curve fitting. Table 10 summarizes the coefficients calculated in each case. It is seen that the coefficients are markedly different, because Ogden model is slightly compressible and therefore it is sensitive to volumetric compression data.

Table 8 Material parameters of the relaxation function $R(t)$, Eq.(16-a)

Sample	Material constants & characteristic time			
	δ^1	δ^2	λ^1(s)	λ^2(s)
1	0.119711	0.107819	1.30735	31.4354
2	0.0646184	0.148176	0.839879	11.9404
3	0.0870321	0.157065	0.730225	12.8898
4	0.113847	0.443071	2.06061	7568071
5	0.0789365	0.229058	1.7787	43.3071
6	0.191661	0.404167	2.388	894404
7	0.0410269	0.0921218	0.308696	10.0431

Table 9 Effect of amount of experimental data on energy function coefficients, Eq.(2)

	Uniaxial data	Uniaxial + biaxial data	Uniaxial+ biaxial + Volumetric compression data
C_1	80.444	1.14558	1.14558
C_2	-91.4945	-0.56398	-0.56398
C_3	12.9236	7.3890	7.3890
C_4	-5.5252	0.2908	0.2908

Table 10 effect of amount of experimental information on the coefficients of Eq.(15)

	Uniaxial data	Uniaxial + biaxial data	Uniaxial+ biaxial + Volumetric compression data
μ_1	1.1691e-7	0.081591	0.00109773
μ_2	0.195871	128.809	0.00343129
α_1	19.563	4.63289	6.8558e-7
α_2	16.5728	0.0001516	3.2820e-8

8. CORRECTION OF MATERIAL CONSTANTS

Strain energy functions used in the above sections for the passive material properties of cardiac muscle, are based partly on observations of tissue microstructure and partly on the results of uniaxial and/or biaxial and volumetric testing of tissue sheets. There is always some doubt, however, that in vitro tests can completely define the in vivo material properties. For these tests on passive tissue in particular, it is impossible during samples preparation to avoid some disruption of perimysial collagen (very thin tissue covering the heart muscles). A judicious combination of in vitro and in vivo tests is therefore needed to determine the material parameters. Finite element model of large deformation heart mechanics can be used for this purpose with clinical Magnetic Resonance Imaging (MRI) tissue tagging measurements. Another important reason for correction and deriving material parameters from clinical intact heart measurements is to assist with the diagnosis of heart disease-many disease states can be characterized by the underlying tissue properties.

The correction process is based on the nonlinear FE Analysis and proceeds as follows:

1. Select an initial set of material parameter estimates (Tables 5-7). This choice is based on the parameters estimated from the uniaxial tension tests.
2. Substitute the current material parameter estimates and predetermined strain field into the stress-strain relations and use the FE ventricular mechanics model to compute the internal stress field and external loads (nodal forces) required to maintain equilibrium.
3. Compute a set of error residuals, based on the differences between the experimentally measured external loads and the nodal forces computed using the model.
4. Minimize these error residuals with respect to the unknown material parameters using a suitable nonlinear optimization technique, such as Levenberg-Marquardt or sequential quadratic programming.

This algorithm is shown schematically in Fig. 9 and could be applied for each deformed state arising from the FE model resulting in several sets of

estimated material parameters with associated sets of error residuals. Overall parameter estimates could be based on simple averages of the individual parameter estimates across the different states of deformation. A better approach may be to combine the sets of error residuals from the various deformed states and minimize this global set of residuals with respect to the unknown material parameters.

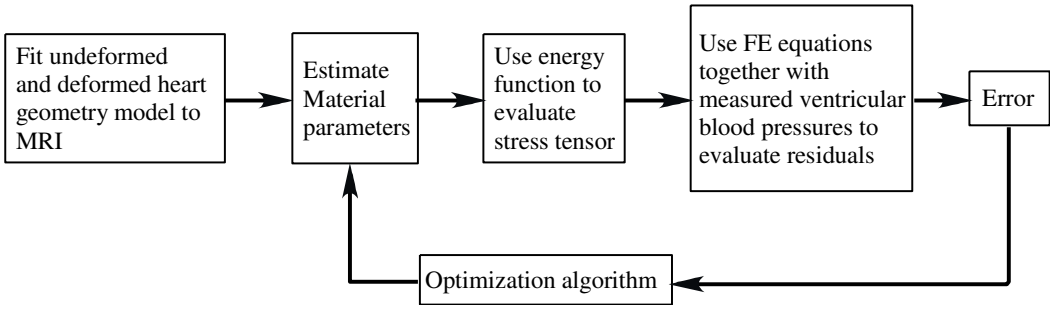

Fig. 9 Estimation algorithms for material parameters

9. CONCLUSIONS

A very precise test rig has been established for making uniaxial and relaxation tests in order to determine mechanical properties of biological tissues. Many tensile and relaxation tests are conducted for heart muscle samples taken from left ventricle of a guinea pig. Muscle material behavior was modeled by a hypo-elastic, hyper-elastic or viscohyperelastic models. Material parameters/ or the constants of the constitutive relation are determined by fitting the experimental data with these models using MATLAB and MRAC optimization tool boxes. Because, the period of the heart cycle is 800 ms and measured relaxation time is very large, the stress relaxation in heart tissues is very small and can be ignored confidently. Therefore viscoelastic model is not appropriate for simulation of the heart mechanics because of large computational time and maybe instability problems would occur. We conclude that Hypoelastic and hyperelastic models simulate the proper mechanical behaviors of the heart muscle and their constitutive relations could be used to regenerate the experimental data. Although uniaxial tension test gives a good initial material properties, but more experimental information is needed to

model the response of heart material under any loading conditions. To overcome this problem and avoid exhaustive experiments and to ensure more precise mechanical properties, an optimization algorithm was proposed to correct and estimate real material parameters from simple uinaxial test and clinical intact heart measurements (MRI or sonography).

ACKNOWLEDGMENT

The author would like to thank Prof. A. Noma, Department of physiology and Biophysics, Graduate School of Medicine, Kyoto University for his useful technical help.

REFERENCES

1. S. Dokos, J. Legrice, H. Smaill, J. Kar and A. Youg, A triaxial-measurement-shear test device for soft biological tissue, J Biomech Eng 122, 471-487 (2000).
2. Y. Le Guennec, N. Peineau, J. A. Argibay, K. G. Mongo and D. Granier, A new method of attachment of isolated mammalian ventricular myocytes for tension recording: length dependence of passive and active tension, J Mol Cell Cardiol 22, 1083-1093 (1990).
3. S. S. Rao, The finite element method in engineering, second edition 1989, Pergamon Press.
4. M. S. Sacks, A Method for planar biaxial mechanical testing that include in-plane shear, J Biomech Eng, vol. 121, 551-555 (1999).
5. J. D. Humphery, R. K. Strumpt and F. C. P. Yin, Determination of a constitutive relation for passive myocardium: part 1 and 2, J Biomech Eng. Vol. 112, 333-346 (1990).
6. L. B. Katsnelson, L. V. Nikitina, and D. chemia , Influence of viscosity on myocardium mechanical activity: a mathematical model, Journal of the theoretical biology, Vol. 230, 385-405 (2004).
7. E. Green and P. M. Naghdi, A general theory of the elastic-plastic continuum, Arch. Rat. Mech. Anal. A18, 251-281, (1965).
8. S. N. Atluri, On constitutive relations at finite strain hypoelasticity and

elastoplasticity with isotropic or kinematic hardening, Comp. Methods Appl. Mech. Eng. Vol. 43, 137-171, (1984).

9. F.J. Carter, et al., Measurements and modeling of the compliance of human and porcine organs, Medical Image Analysis, 5 (2001) 231-236
10. B.K. Tay, et al., Measurement of In-vivo Force Response of Intra-Abdominal Soft Tissues for Surgical Simulation, Proceedings of Medicine Meets Virtual Reality 02/10, J.D. Westwood, et al. (Eds.), Newport Beach, CA. IOS Press. 514-519. 23-26 Jan 2002.
11. M.P. Ottensmeyer, In vivo measurement of solid organ visco-elastic properties, Proceedings of Medicine Meets Virtual Reality 02/10, J.D. Westwood, et al. (Eds.), Newport Beach, CA. IOS Press. 328-333. 23-26 Jan 2002.
12. Brower, et al., Measuring In Vivo Animal Soft Tissue Properties for Haptic Modeling in Surgical Simulation, Medicine Meets Virtual Reality 2001, Studies in Health Technology and Informatics, 81, Newport Beach, CA (24-27 Jan 2001) 69–74
13. J.D. Brown, et al., Computer-Controlled Motorized Endoscopic Grapser for In Vivo Measurement of Soft Tissue Biomechanical Characteristics, Proceedings of Medicine Meets Virtual Reality 02/10, J.D. Westwood, et al. (Eds.), Newport Beach, CA. IOS Press. 71-73. 23-26 Jan 2002.
14. J. Gross, et al., Modelling Viscoelasticity for Interactive Surgery Simulation. In course syllabus of, and poster presented at Medicine Meets Virtual Reality 02/10, Newport Beach, CA. 70-71. 23-26 Jan 2002.
15. L. Gao, et al., “Imaging of the elastic properties of tissue—a review,” Ultrasound in Medicine and Biology, 22(8) (1996) 959-977
16. M. Suga, et al., Sensible Human Projects: Haptic Modeling and Surgical Simulation Based on Measurements of Practical Patients with MR Elastography – Measurement of Elastic Modulus. Proceedings of Medicine Meets Virtual Reality 2000, J.D. Westwood, et al. (Eds.), Newport Beach, CA. IOS Press. 334-340. 27-30 Jan 2000.
17. A. J. M. Spencer, Continuum Mechanics, Longman Group Ltd., London (1980).

18. M. A. Hassan and A. Amano, Study of the Effective Boundary conditions in Finite Element simulation of Heart mechanics, Kyoto University International Symposium on Leading Project for Biosimulation, 2004.
19. P.J. Hunter and B.H. Smaill, The analysis of cardiac function: a continuum approach, Prog Biophys Molec Biol. 52(1988) 101-164.

قياس الخواص المرنة والمرنة اللزجة الغير خطية لعضلة البطين الأيسر لقلب خنزير غيني

تعتبر الخواص الميكانيكية لأنسجة عضلات القلب هي المشكلة الجوهرية فى عملية المحاكاة الحيوية لميكانيكا القلب باستخدام العناصر المحدوده. يقوم هذا البحث بدراسة عملية وتحليلية للخواص المرنة والخواص المرنة اللزجة الغير خطية لعضلة قلب الخنزير الذي يشبه كثيراً فى خواصه وأدائه لقلب الإنسان. استخدمت النتائج العملية لاختبارات الشد الدقيق فى اتجاه واحد لتعيين ثوابت النمط ذو المرونة الضئيلة الغير خطى (Hypoelastic). كما أنها استخدمت فى تعيين ثوابت النمط الغير خطى ذو المرونة الزائدة (Hyperelsatic) والذي يمثل بدالة طاقة انفعالية ذات مرونة زائدة (hyperelastic strain energy function) . وبالنسبة للخواص اللزجة فقد تم تعيينها من اختبارات الارتخاء. أما بالنسبة للخواص المرنة اللزجة تم تحليليها باستخدام دالة طاقة توصف السلوك الانفعالي اللزج والتي تعتمد على نظرية الفصل متعدد الطبقات Multiplicative Decomposition Theory لحاصل ضرب دالة طاقة انفعالية ذات مرونة زائدة مع دالة ارتخاء ويكون الناتج فى صورة متسلسلة (Prony series).

أستخدم ألـ (non-linear fitting and optimization) لحساب الثوابت لكل نوع من أنواع السلوك الثابت. و قد وجد من خلال الدراسة الاكلينيكية للقلب أن الخواص الغيرخطيه ذواتاً المرونة الضئيلة والزائدة (Hypoelastic & hyperelastic) هي الأمثل لتوصيف استجابة أنسجة عضلة القلب لأحمال الضغط والشد. أما بالنسبة للسلوك اللزج فيمكن إهماله لأن ثابت وقت التراجع (Relaxation time constant) المحسوب من منحى الارتخاء كان كبير جداً جداً (700s) بالنسبة لزمن دورة حركة القلب(heart beating cycle) الذي كان (800 ms). وأخيرا لكي نحصل على أكثر دقة للخواص الميكانيكية عن طريق الـ Optimization الذي يعتمد على تقليل الخطأ بين حركة القلب باستخدام العناصر المحدودة وحركته الحقيقية المأخوذة من أشعة الرنين المغناطيسي وذلك بتعديل القيم العملية. هذه الطريقة المقترحة يمكن بواسطتها تحديد الخواص الميكانيكية الحقيقية لعضلة القلب عن طريق بعض القياست العملية كقيمة مبدئية واستخدام العناصر المحدودة وأشعة الرنين المغناطيسي.

هذا البحث ذو فائدة كبيرة فى مجال الهندسة الطبية وبخاصة ميكانيكا القلب حيث يمكننا من تحديد الخواص الميكانيكية الحقيقية لعضلة القلب والتي تساعد بدورها فى تطوير مادة تستخدم فى صناعة القلب الاصطناعي.